Validation Note

ATLAS-EXOT-2018-06 analysis in the MadAnalysis 5 framework

1 Introduction

This note describes the implementation of the analysis ATLAS-EXOT-2018-06 [1] in MADANALYSIS 5 [2, 3] that is now available in the Public Analysis Database [4]. This analysis targets the search for new physics in final states with an energetic jet and large missing transverse momentum. It uses 139 fb^{-1} of data at a center-of-mass energy of 13 TeV, collected in the period 2015–2018 with the ATLAS detector at the Large Hadron Collider (LHC). Events are required to have at least one jet with transverse momentum above 150 GeV (or 200 GeV) and no reconstructed leptons (electrons, muons or taus) or photons. The final-state signature featuring at least one energetic jet, large p_T^{miss} and no leptons constitutes a distinctive signature for new physics BSM at colliders. This signature has been extensively studied at the LHC in the context of searches for :

1. large extra spatial dimensions,
2. supersymmetric particles in several compressed scenarios,
3. models with pair-produced weakly interacting massive particles as candidates for dark matter,
4. new theoretical scenarios with axion-like particles,
5. signals from models inspired by dark energy with new scalar particles in the final state.

Compared to previous publications using only 3.2 fb^{-1}[5] and 36.1 fb^{-1}[6] of data, the analysis includes a number of improvements in the signal selection and the background determination leading to enhanced sensitivity.

The ATLAS collaboration made available substantial additional data via HepData at `https://www.hepdata.net/record/ins1847779`, including in particular detailed cut-flows, tables and exclusion curves as well as digitised information on the figures.

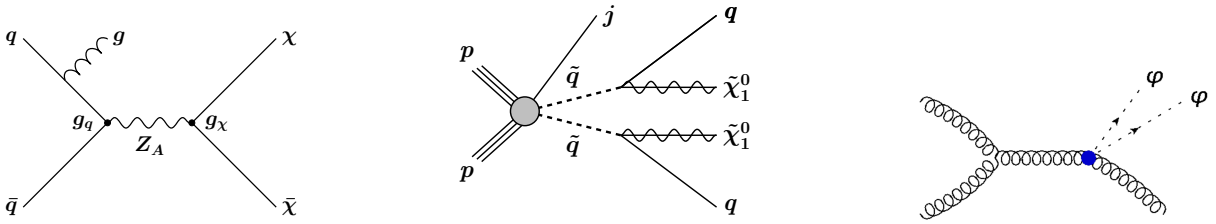

(a) (b) (c)

FIGURE 1 – Representative diagrams fro the processes relevant to this analysis : a Pair production of weakly interacting massive particles χ through a mediator Z_A with axial-vector couplings exchanged in the s-channel. b Pair production of squarks that decay through $\tilde{q} \to q + \tilde{\chi}_1^0$. The presence of a jet from initial-state radiation is indicated for illustration purposes. c Pair production of dark-energy scalar fields φ in association with an energetic jet in the final state.

2 Description of the analysis

This ATLAS analysis targets a final-state containing at least one very energetic jet that is assumed to originate from initial state radiation, as well as a certain amount of missing transverse energy E_T^{miss}.

2.1 Object definition in the ATLAS paper

Jets are reconstructed by using the anti-k_t jet algorithm [7], as provided by the FASTJET [8] toolkit, with the radius parameter $R = 0.4$. Only those jets with $p_T > 20$ GeV and $|\eta| < 2.8$ are considered in the analysis. Jets with $p_T > 30$ GeV and $|\eta| < 2.5$ are identified as jets containing b-hadrons (b-jets) according to a b-tagging working point that is in average 60% efficient [9].

Next, an overlap removal procedure is applied to jets, electrons, muons, taus and photons.

Electrons are initially required to have $p_T > 7$ GeV and $|\eta| < 2.47$, and to satisfy the 'Loose' track selection criteria [10], including a requirement on the match between the track and the primary vertex, which requires the longitudinal impact parameter $|z_0| \sin\theta$ to be less than 0.5 mm. Overlaps between identified electrons and jets with $p_T > 30$ GeV in the final state are resolved. Jets are discarded if they are not b-tagged and their separation $\Delta R = \sqrt{(\Delta\eta)^2 + (\Delta\phi)^2}$ from an identified electron is less than 0.2. The electrons separated by ΔR between 0.2 and 0.4 from any remaining jet are removed.

Muon are required to pass 'Medium' identification requirements [11], and to have $p_T > 7$ GeV and $|\eta| < 2.5$. As in the case of electrons, the muon track is required to have $|z_0| \sin\theta < 0.5$ mm. Jets with $p_T > 30$ GeV and fewer than three tracks with $p_T > 500$

MeV associated with them are discarded if their separation from an identified muon is less than 0.4.

Hadronically decaying τ-lepton candidates are formed by combining information from the calorimeters and inner tracking detectors. The τ-lepton reconstruction algorithm [12] is seeded by reconstructed jets with $p_T > 10$ GeV and $|\eta| < 2.5$, and the reconstructed energies of the τ-lepton candidates are corrected to the τ-lepton energy scale. They are required to pass 'Loose' identification requirements [13], to have $p_T > 20$ GeV and $|\eta| < 2.5$, and to have one or three associated charged tracks. τ-leptons close to electrons or muons ($\Delta R < 0.2$) are removed. Any jet within $\Delta R = 0.2$ of a τ-lepton is removed.

Photons are required to pass 'Tight' identification requirements [10], and to have $p_T > 10$ GeV and $|\eta| < 2.37$. Photons are discarded if their separation ΔR from an identified muon or electron is less than 0.4.

The vector missing transverse momentum p_T^{miss} is reconstructed from the negative vectorial sum of the transverse momenta of electrons, muons, τ-lepton, photons, and jets with $p_T > 20$ GeV and $|\eta| < 4.5$.

2.2 Event pre-selection

A cut over all the events, $E_T^{miss} > 150$ GeV, is implemented in order to reproduce the initial simulated sample generated with a minimum transverse momentum of 150 GeV done in the ATLAS paper. It will not appear in the final code. Event preselection imposes the presence of a significant amount of missing energy, $E_T^{miss} > 200$ GeV, a leading jet with $p_T > 150$ GeV and $|\eta| < 2.4$, and up to three additional jets with $p_T > 30$ GeV and $|\eta| < 2.8$.

Separation in the azimuthal angle of $\Delta\phi(\text{jet}, p_T^{miss}) > 0.4\,(0.6)$ between the missing transverse momentum direction and each selected jet is required for events with $E_T^{miss} >$ 250GeV (200GeV $< E_T^{miss} \leq$ 250GeV) to reduce the multijet background contribution.

2.3 Signal Regions and summary

The analysis strategy is twofold, depending on the selection cut on the missing transverse energy. Inclusive bins (named "IM") are used for a model-independent interpretation of the search results, while the full set of exclusive bins (named "EM) are used for the interpretation within different models of new physics.

In a first series of thirteen signal regions (EM0, EM1, . . ., EM12), the analysis considers exclusive missing transverse energy selection, $E_{threshold}^{min} < E_T^{miss} < E_{threshold}^{max}$, where the 13 different thresholds range from 200 GeV to 1200 GeV. In a second series of thirteen signal regions (IM0, IM1, . . ., IM12), it considers instead inclusive missing transverse energy

TABLE 1 – Intervals and labels of the E_T^{miss} bins used for the signal region.

Exclusive (EM)	EM0	EM1	EM2	EM3	EM4	EM5	EM6
E_T^{miss} [GeV]	200–250	250–300	300–350	350–400	400–500	500–600	600–700
	EM7	EM8	EM9	EM10	EM11	EM12	
	700–800	800–900	900–1000	1000–1100	1100–1200	>1200	
Inclusive (IM)	IM0	IM1	IM2	IM3	IM4	IM5	IM6
E_T^{miss} [GeV]	>200	>250	>300	>350	>400	>500	>600
	IM7	IM8	IM9	IM10	IM11	IM12	
	>700	>800	>900	>1000	>1100	>1200	

SR	Cut
	Total evts (truth E_T^{miss} > 150 GeV)
	Trigger
	Event cleaning
	Lepton veto
Pre–selection	$N_{jets} \leq 4$
	$\min \Delta\Phi\left(\text{jets}, E_T^{miss}\right)$ cut
	Lead. Jet quality requirements
	Lead. Jet p_T > 150 GeV and lead. Jet $\lvert\eta\rvert$ < 2.4
	E_T^{miss} > 200 GeV
EM0	200 GeV < E_T^{miss} ≤250 GeV
EM1	250 GeV < E_T^{miss} ≤300 GeV
EM2	300 GeV < E_T^{miss} ≤350 GeV
EM3	350 GeV < E_T^{miss} ≤400 GeV
EM4	400 GeV < E_T^{miss} ≤500 GeV
EM5	500 GeV < E_T^{miss} ≤600 GeV
EM6	600 GeV < E_T^{miss} ≤700 GeV
EM7	700 GeV < E_T^{miss} ≤800 GeV
EM8	800 GeV < E_T^{miss} ≤900 GeV
EM9	900 GeV < E_T^{miss} ≤1000 GeV
EM10	1000 GeV < E_T^{miss} ≤1100 GeV
EM11	1100 GeV < E_T^{miss} ≤1200 GeV
EM12	E_T^{miss} >1200 GeV

FIGURE 2 – Summary of all the cuts and "EM" Signal Regions (SR)

selections, $E_T^{miss} > E_{threshold}$ with the same thresholds range. These signal regions (SRs) are summed up in Table 1.

Figure 2 presents all the cuts done for all the SRs and the specific cuts for each "EM" SRs (from the ATLAS paper).

3 Validation

Two principal types of results are presented : model-independent and model-dependent exclusion limits. We will focus essentially on the squark-pair production case.

3.1 Generation of signal events

Different models of squark-pair production are considered : stop-pair production with $\tilde{t}_1 \to c + \tilde{\chi}_1^0$, stop-pair production with $\tilde{t}_1 \to b + ff' + \tilde{\chi}_1^0$, sbottom-pair production with $\tilde{b}_1 \to b + \tilde{\chi}_1^0$, and squark-pair production with $\tilde{q} \to q + \tilde{\chi}_1^0$ ($q = u, d, c, s$). The results are translated into exclusion limits as a function of the squark mass for different neutralino masses. For our validation procedure, we considered first the $\tilde{t}_1 \to b + ff' + \tilde{\chi}_1^0$ decay channel. The additional case considered is the $\tilde{t}_1 \to c + \tilde{\chi}_1^0$ decay channel (for the second validation plot).

Signal events have been generated with MADGRAPH5_AMC@NLO[14] v.3_4_2 and Pythia 8 [15] for the hard scattering matrix elements and the simulation of the parton showering and hadronization, respectively. The merging scale as been set, for each point, to $Q^{match} = M_{\tilde{t}}/4$ GeV for a MADGRAPH5 xqcut parameter set to 100 GeV. MSSM [16, 17] within MADGRAPH5_AMC@NLO has been used to reproduce the wanted decay. More specifically, we used a class of simplified models where the Standard Model is extended by a neutralino and a stop to produce the two decay channels considered for the validation. To match the cutflows provided, I simulated 100k events at leading order in MADGRAPH5_AMC@NLO, which after merging and passing to Pythia8 give 90k merged events.

For the validation we used ma5_expert (`https://github.com/MadAnalysis/ma5_expert`), MadAnalysis 5 output interpreter for expert mode that parses the cutflow and histogram collections and constructs it with an interactable interface.

SR	Cut	DMA_1_2000		DMP_1_350		SS_direct_900_895		TT_bffN_450_443		BB_direct_500_300		TT_directCC_600_593		DE_C2_M1000		H(inv)	
	Total evts (truth E_T^{miss} > 150 GeV)	10282	100.00%	199254	100.00%	5750	100.00%	39598	100.00%	95200	100.00%	8857	100.00%	102275	100.00%	406282	100.00%
	Trigger	10101	98.23%	193342	97.03%	5651	98.27%	38851	98.11%	93802	98.53%	8694	98.15%	100300	98.07%	388725	95.68%
	Event cleaning	10091	98.14%	193094	96.91%	5642	98.11%	38783	97.94%	93679	98.40%	8677	97.97%	100135	97.91%	387588	95.40%
	Lepton veto	9788	95.19%	187094	93.90%	5435	94.51%	37547	94.82%	89103	93.60%	8352	94.29%	95799	93.67%	363894	88.57%
Pre–selection	$N_{jets} \leq 4$	9455	91.95%	176978	88.82%	5142	89.43%	35412	89.43%	74701	78.47%	7924	89.46%	86034	84.12%	339112	83.47%
	$\min \Delta\Phi\left(\text{jets}, E_T^{miss}\right)$ cut	9104	88.54%	168962	84.80%	4838	84.14%	33319	84.14%	66128	69.46%	7463	84.26%	78632	76.88%	324583	79.89%
	Lead. Jet quality requirements	8963	87.17%	160714	80.66%	4687	81.50%	31870	80.48%	64964	68.24%	7197	81.26%	76516	74.81%	306825	75.52%
	Lead. Jet p_T > 150 GeV and lead. Jet $\|\eta\| < 2.4$	6642	64.60%	90366	45.35%	3508	61.00%	23134	58.42%	48148	50.58%	5379	60.73%	56942	55.68%	160684	39.55%
	E_T^{miss} > 200 GeV	5317	51.71%	60133	30.18%	3018	52.48%	18801	47.48%	37203	39.08%	4444	50.17%	49799	48.69%	100172	24.66%
EM0	200 GeV < E_T^{miss} ≤250 GeV	1346	13.09%	25162	12.63%	562	9.77%	4488	11.34%	11972	12.58%	968	10.93%	8394	8.21%	45920	11.30%
EM1	250 GeV < E_T^{miss} ≤300 GeV	1045	10.17%	15549	7.80%	536	9.32%	3789	9.57%	11167	11.73%	804	9.08%	8282	8.10%	26061	6.41%
EM2	300 GeV < E_T^{miss} ≤350 GeV	771	7.49%	8648	4.34%	416	7.23%	2857	7.21%	6670	7.01%	662	7.48%	6801	6.65%	13409	3.30%
EM3	350 GeV < E_T^{miss} ≤400 GeV	552	5.36%	4717	2.37%	316	5.50%	2111	5.33%	3266	3.43%	493	5.57%	5424	5.30%	6831	1.68%
EM4	400 GeV < E_T^{miss} ≤500 GeV	684	6.65%	4034	2.02%	439	7.63%	2618	6.61%	2670	2.80%	640	7.23%	7604	7.44%	5266	1.30%
EM5	500 GeV < E_T^{miss} ≤600 GeV	371	3.61%	1303	0.65%	267	4.65%	1352	3.41%	870	0.91%	379	4.28%	4711	4.61%	1703	0.42%
EM6	600 GeV < E_T^{miss} ≤700 GeV	212	2.06%	444	0.22%	177	3.08%	712	1.80%	332	0.35%	222	2.50%	2981	2.91%	578	0.14%
EM7	700 GeV < E_T^{miss} ≤800 GeV	126	1.22%	156	0.08%	110	1.92%	393	0.99%	132	0.14%	112	1.27%	1950	1.91%	225	0.06%
EM8	800 GeV < E_T^{miss} ≤900 GeV	79	0.77%	67	0.03%	71	1.23%	204	0.52%	61	0.06%	64	0.72%	1236	1.21%	89	0.02%
EM9	900 GeV < E_T^{miss} ≤1000 GeV	48	0.47%	28	0.01%	48	0.84%	122	0.31%	35	0.04%	40	0.45%	801	0.78%	48	0.01%
EM10	1000 GeV < E_T^{miss} ≤1100 GeV	29	0.28%	12	0.01%	28	0.50%	58	0.15%	14	0.02%	26	0.29%	542	0.53%	21	0.01%
EM11	1100 GeV < E_T^{miss} ≤1200 GeV	19	0.18%	7	0.00%	17	0.30%	42	0.11%	6	0.01%	12	0.13%	348	0.34%	9	0.00%
EM12	E_T^{miss} >1200 GeV	35	0.34%	6	0.00%	29	0.51%	55	0.14%	7	0.01%	21	0.24%	725	0.71%	12	0.00%

FIGURE 3 – Cutflow of several signal benchmarks. A pre-cut on the truth E_T^{miss} at 150 GeV is applied. In our validation we are only interested in the TT_bffN_450_443 column which corresponds to the $\tilde{t}_1 \rightarrow b + ff' + \tilde{\chi}_1^0$ decay channel with $m_{\tilde{t}_1} = 450$ GeV and $m_{\tilde{\chi}_1^0} = 443$ GeV

3.2 Cutflow table comparison

The HepData file, reproduced in Figure 3, gives us the cutflow table of several signal benchmarks. A pre-cut on the truth E_T^{miss} at 150 GeV is applied. In our validation we are only interested in the TT_bffN_450_443 column which corresponds to the $\tilde{t}_1 \rightarrow b + ff' + \tilde{\chi}_1^0$ decay channel with $m_{\tilde{t}_1} = 450$ GeV and $m_{\tilde{\chi}_1^0} = 443$ GeV.

In Figure 4 is presented the Cutflow table of the $\tilde{t}_1 \rightarrow b + ff' + \tilde{\chi}_1^0$ decay channel with $m_{\tilde{t}_1} = 450$ GeV and $m_{\tilde{\chi}_1^0} = 443$ GeV. There are two columns : one for ATLAS results and the other for the results from this recasting.

1. ϵ corresponds to the efficiencies calculated thanks to the cutflow tables : $\epsilon = \frac{\text{number of events after the cut}}{\text{total number of events}}$
2. δ corresponds to the Monte-Carlo uncertainty calculated on the efficiencies thanks to ma5expert,
3. R_{gap} is the relative gap on efficiencies : $R_{gap} = |\frac{\epsilon_{ATLAS} - \epsilon_{recasting}}{\epsilon_{ATLAS}}|$

We obtain good results in this comparison with the ATLAS analysis, with low R_{gap} (from 1 to 25 %). To validate these good results, two plots of two different decay channel have been done.

	ATLAS			MadAnalysis 5-SFS				
	Events	ε [%]	ε_{cut} [%]	Events	ε [%]	δ [%]	ε_{cut} [%]	R_{gap} [%]
Initial (truth $E_T^{miss} > 150$ GeV)	39598	-	100	89529	-	0.17	100	-
Lepton veto	37547	94.82	94.82	85417	95.41	0.17	95.41	0.62
$N_{jets} \leq 4$	35412	89.43	94.31	76195	85.11	0.18	89.20	4.38
$\min[\Delta\phi(jets, E_T^{miss})]$ cut	33319	84.14	94.10	69253	77.35	0.18	91.00	8.07
Leading jet > 150 GeV and $\lvert\eta\rvert < 2.4$	23134	58.42	69.43	47157	52.67	0.20	68.10	9.84
$E_T^{miss} > 200$ GeV	18801	47.48	81.30	39183	43.77	0.20	83.10	7.81
EM0	4488	11.34	-	8509	9.50	0.22	-	16.23
EM1	3789	9.57	-	7946	8.88	-	-	7.21
EM2	2857	7.21	-	6226	6.95	-	-	3.61
EM3	2111	5.33	-	4621	5.16	-	-	3.19
EM4	2618	6.61	-	5847	6.53	-	-	1.21
EM5	1352	3.41	-	2895	3.23	-	-	5.28
EM6	712	1.80	-	1501	1.67	-	-	7.22
EM7	393	0.99	-	719	0.80	-	-	19.19
EM8	204	0.52	-	408	0.46	-	-	11.54
EM9	122	0.31	-	207	0.23	-	-	25.80
EM10	58	0.15	-	124	0.14	-	-	6.67
EM11	42	0.11	-	77	0.09	-	-	18.18
EM12	55	0.14	-	103	0.11	-	-	21.43

ε : efficiency
ε_{cut} : efficiency cut by cut
δ : MC uncertainty
R_{gap} : relative gap on efficiencies

FIGURE 4 – Cutflow table comparison of the $\tilde{t}_1 \to b + ff' + \tilde{\chi}_1^0$ decay channel with $m_{\tilde{t}_1} = 450$ GeV and $m_{\tilde{\chi}_1^0} = 443$ GeV. The ATLAS column corresponds to the cutflow table given by the ATLAS collaboration team and the MadAnalysis 5-SFS column corresponds to the results obtained within the recasting.

3.3 Validation plots

Even with the validation given by the ATLAS cutflow comparison with our recasting, we have decided to validate our reimplementation by reproducing the ATLAS excluded regions at the 95% CL in the $(\tilde{t}_1, \tilde{\chi}_1^0)$ mass plane for the decay channel $\tilde{t}_1 \to c + \tilde{\chi}_1^0$ ($\mathcal{B} = 100\%$) and the decay channel $\tilde{t}_1 \to b + f f^{'} + \tilde{\chi}_1^0$ ($\mathcal{B} = 100\%$).

Our results are presented in Fig. 5 in which we superimpose the exclusion contour obtained with MADANALYSIS 5 (green) with the official ATLAS one (black). An excellent degree of agreement is observed.

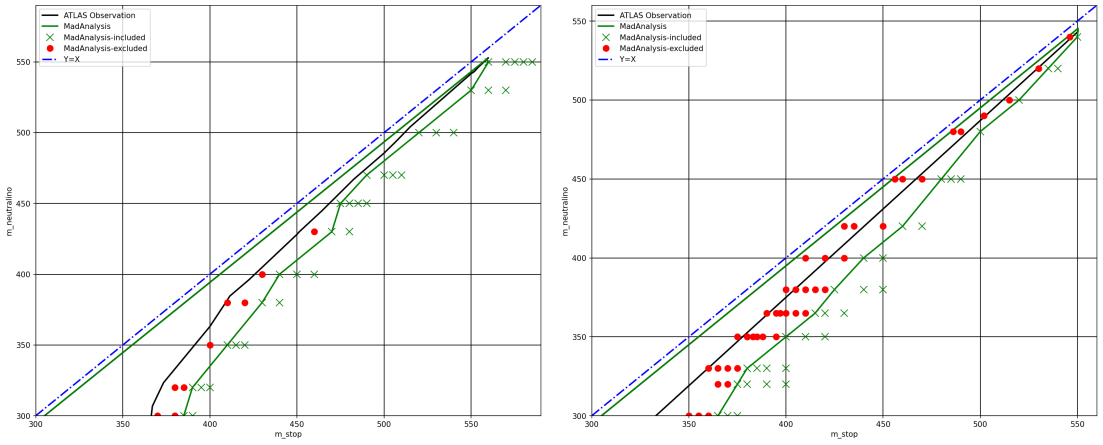

(a) (b)

FIGURE 5 – Excluded regions at the 95% CL in the $(\tilde{t}_1, \tilde{\chi}_1^0)$ mass plane for the decay channel $\tilde{t}_1 \to c + \tilde{\chi}_1^0$ (left) and the decay channel $\tilde{t}_1 \to b + f f^{'} + \tilde{\chi}_1^0$ (right). The green marks are for points within the 95% CL (called "included"). The red marks are for points without 95% CL (called "excluded"). The black line comes from ATLAS analysis observation while the green line comes from the recasting. The gap between the two lines is small, we observe a good degree of agreement.

4 Summary

We have implemented the ATLAS-EXOT-2018-06 analysis in the MADANALYSIS 5 framework, an analysis targeting the search for new physics in final states with an energetic jet and large missing transverse momentum and in 139 fb^{-1} at a center-of-mass energy of 13 TeV collected with the ATLAS detector at the LHC. We have validated our recasting in reproducing the cutflow table for a specific decay channel and the exclusion curve provided by ATLAS for two separate decay channels. We have obtained good agreement, so that our reimplementation has been considered as validated. The code is available online from the MadAnalysis 5 dataverse, at `https://doi.org/10.14428/DVN/REPAMM`.

Références

[1] ATLAS collaboration. Search for new phenomena in events with an energetic jet and missing transverse momentum in pp collisions with the atlas detector. *Physical Review D*, 103(11), jun 2021.

[2] Eric Conte, Benjamin Fuks, and Guillaume Serret. MadAnalysis 5, a user-friendly framework for collider phenomenology. *Computer Physics Communications*, 184(1) :222–256, jan 2013.

[3] Jack Y. Araz, Benjamin Fuks, and Georgios Polykratis. Simplified fast detector simulation in MadAnalysis 5. *The European Physical Journal C*, 81(4), apr 2021.

[4] B. Dumont, B. Fuks, S. Kraml, S. Bein, G. Chalons, E. Conte, S. Kulkarni, D. Sengupta, and C. Wymant. Toward a public analysis database for LHC new physics searches using MADANALYSIS 5. *The European Physical Journal C*, 75(2), feb 2015.

[5] ATLAS collaboration. Search for new phenomena in final states with an energetic jet and large missing transverse momentum in pp collisions using the atlas detector. *Physical Review D*, 94(3), aug 2016.

[6] ATLAS collaboration. Search for dark matter and other new phenomena in events with an energetic jet and large missing transverse momentum using the atlas detector. *Journal of High Energy Physics*, 2018(1), jan 2018.

[7] Matteo Cacciari, Gavin P Salam, and Gregory Soyez. The anti-jet clustering algorithm. *Journal of High Energy Physics*, 2008(04) :063–063, apr 2008.

[8] Matteo Cacciari, Gavin P. Salam, and Gregory Soyez. FastJet user manual. *The European Physical Journal C*, 72(3), mar 2012.

[9] Optimisation of the ATLAS *b*-tagging performance for the 2016 LHC Run. Technical report, CERN, Geneva, 2016. All figures including auxiliary figures are available at https ://atlas.web.cern.ch/Atlas/GROUPS/PHYSICS/PUBNOTES/ATL-PHYS-PUB-2016-012.

[10] ATLAS collaboration. Electron and photon performance measurements with the ATLAS detector using the 2015–2017 LHC proton-proton collision data. *Journal of Instrumentation*, 14(12) :P12006–P12006, dec 2019.

[11] ATLAS collaboration. Muon reconstruction performance of the ATLAS detector in proton–proton collision data at $$\sqrt{s}$$ s =13 TeV. *The European Physical Journal C*, 76(5), may 2016.

[12] ATLAS collaboration. Identification and energy calibration of hadronically decaying tau leptons with the ATLAS experiment in pp collisions at $$\sqrt{s}=8$$ s = 8 $$\, \hbox {TeV}$$ TeV. *The European Physical Journal C*, 75(7), jul 2015.

[13] Reconstruction, Energy Calibration, and Identification of Hadronically Decaying Tau Leptons in the ATLAS Experiment for Run-2 of the LHC. Technical report, CERN, Geneva, 2015. All figures including auxiliary figures are available at https ://atlas.web.cern.ch/Atlas/GROUPS/PHYSICS/PUBNOTES/ATL-PHYS-PUB-2015-045.

[14] J. Alwall, R. Frederix, S. Frixione, V. Hirschi, F. Maltoni, O. Mattelaer, H.-S. Shao, T. Stelzer, P. Torrielli, and M. Zaro. The automated computation of tree-level and next-to-leading order differential cross sections, and their matching to parton shower simulations. *Journal of High Energy Physics*, 2014(7), jul 2014.

[15] Torbjörn Sjöstrand, Stefan Ask, Jesper R. Christiansen, Richard Corke, Nishita Desai, Philip Ilten, Stephen Mrenna, Stefan Prestel, Christine O. Rasmussen, and Peter Z. Skands. An introduction to PYTHIA 8.2. *Computer Physics Communications*, 191 :159–177, jun 2015.

[16] Neil Christensen, Priscila de Aquino, Celine Degrande, Claude Duhr, Benjamin Fuks, Michel Herquet, Fabio Maltoni, and Steffen Schumann. A comprehensive approach to new physics simulations. *The European Physical Journal C*, 71(2), feb 2011.

[17] Claude Duhr and Benjamin Fuks. A superspace module for the FeynRules package. *Computer Physics Communications*, 182(11) :2404–2426, nov 2011.